JEEMECS (Journal of Electrical Engineering, Mechatronic and Computer Science ISSN 2614-4859
Vol. 5, No. 2, August 2022, pp. 77-90

Efficiency of the Position Tracking Photovoltaics using Microcontroller Atmega

Anggara Trisna Nugraha [a,1,*], Moch Fadhil Ramadhan [b,2], Muhammad Jafar Shiddiq [b,3]

[1] Marine Electrical Engineering Shipbuilding Institute of Polytechnic Surabaya, Jl. Teknik Kimia Keputih Sukolilo, Surabaya 60111, Indonesia
[2] Automation Engineering Shipbuilding Institute of Polytechnic Surabaya, Jl. Teknik Kimia Keputih Sukolilo, Surabaya 60111, Indonesia
[1] anggaranugraha@ppns.ac.id *;
[*] corresponding author

Keywords
Photovoltaics
Sunshine Tracker
Microcontroller
Atmega16

ABSTRACT

So far, solar cells are known to have many weaknesses in terms of installation and position to the sun, so that the performance of solar cells on rechargeable batteries is less than optimal. Therefore, additional tools are needed to support these solar cells so that they can work optimally and produce bigger currents. Compare a sunlight tracker with an LDR system, and compare a sunlight tracker with a direct sunlight sensor with a passive system. Atmega16 is used as a control motor and automatic charger, LDR is used as a sunshine receiver, and a DC motor and a stepper are used as a sunshine indicator player. The solar cell used has a capacity of 20 WP. The automatic filling system uses a microcontroller to increase the cost and efficiency of installation. After that, the two systems will be compared first to find out the difference in power generated by the solar cell system using a tracer and a passive tracer. Using a tracking system will collect data for a week, while using a passive system will collect data for a week. By using the result data to be analyzed, the system can be analyzed and compared, and its efficiency can be determined. The solar cell tracking system is expected to increase battery charge faster than passive locations.

1. Introduction

Electricity is a necessity that is indispensable in everyday life as well as in the industrial and commercial world. Because the equipment in everyday life uses a large number of electrical energy systems, it is easy to use and operate [1].

Currently, most of the generators used for generators still use coal fuel, and the rest use geothermal power plants, diesel power plants (PLTD), and solar power plants (PLTS). Even in the United States, the energy is extraordinary. Still converted into electrical energy. Large scale. Very small [2].

Indonesia is a tropical country with two seasons, and in four seasons, Indonesia still has around 8 hours of sunshine a day. Indonesian sunshine can be used as a power plant through PHOTOVOLTAIC (solar cells) media, and can also be used as a converter of renewable energy.

Installing a passive system is not the best way to absorb solar energy, because when the sun is still very hot and the position of the solar cell is not completely at 90o, the solar cell still cannot absorb solar energy.

Therefore, it is necessary to change the solar energy collection system to make it more optimal. In this research will be carried out "Analysis of the Efficiency of the Solar Tracker using Atmega 16". The method of using solar panels directly can continuously absorb the maximum energy from sunlight, which is automatically controlled by the ATMEGA16 microcontroller, and the light sensor media can be used as detectors of irregular and rotating sunlight. The motor microcontroller acts as a mechanical drive for the solar cell holder and stops running until it reaches the sun position 90°.

2. The Proposed Method/Algorithm

Explanations and materials used in this study, among others Solar Cell, Light Dependent Resistor (LDR), DC motor, Current Sensor, ATMEGA 16, LCD, IC Driver Motor L293D.

2.1. Solar Cell

The working principle of solar cells is based on the P-N connection concept. When current flows through the n-type layer (electrons) and the p-type layer (holes), the unit consisting of p-type and n-type semiconductors forms a p-n connection, an anti-reflection layer and a metal substrate [10].

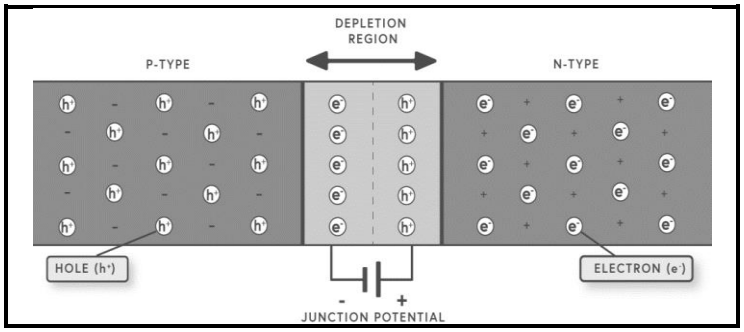

Fig. 1. The structure of the P-N junction on the solar silicon cell [3]

N-type semiconductors are obtained by filling silicon with group V elements, which have more valence electrons than the surrounding atoms. On the other hand, a p-type semiconductor is obtained by filling in group III, and its valence electrons are deformed in comparison with the surrounding atoms [11]. When these two materials come into contact, the excess electrons will diffuse from the N-type to the P-type. In this way, the region containing N will be positively charged, and the region doped P will be negatively charged. The electric field generated between the two electrons forces them to return to the -N region and allows the hole to enter the P region [3]. In this process, a P-N junction is formed. By adding metal contacts in the P and N regions, diodes can be formed.

2.2. Light Dependent Resistor (LDR)

LDR (Photosensitive Resistor) is a type of resistor whose resistance changes according to the intensity of light received. The results of the LDR resistance measurement show that the greater the light received, the smaller the resistance, conversely, the smaller the light received, the greater the resistance. The LDR resistance in dark places can reach 10MΩ, while the LDR resistance in bright places drops to 150Ω. LDR is made of semiconductor materials, such as cadmium sul-fidatr [4]. With this material, the energy from falling light will cause more charge to be released or the current to increase. This means reduced material resistance.

2.3. DC Motor

A DC motor is an electrical device that can convert electricity into mechanical quantities through an electromagnetic field. DC motors require DC voltage to supply power to the stator winding (the non-rotating part of the winding) and the rotor (the rotating part of the winding) to generate an electromagnetic field to make it rotate [12].

The working principle of a direct current (DC) motor is to use a brush (commutator) to reverse the positive voltage so that it can reverse the current through the armature coil which rotates in the permanent magnetic field. Battery power flowing through the two brush sections (commutator) is connected to both ends of the rotor winding. For the DC motor rotation process to be perfect, the power supply voltage must be greater than the legal moving voltage, and rotation will occur by supplying current to the armature coil which is protected by a magnetic field [13].

The DC motor used in this study is the MG 996 DC motor which has a higher power level because it uses an additional gearbox to control the torque ratio and motor speed [14].

2.4. Current Sensor

When charging the battery via solar cells, a current sensor is required to monitor the battery current and act as an automatic vehicle controller [15], which is then sent to the microcontroller. The sensor used here is the ACS712 Hall-effect sensor, which can replace the relatively small parallel

resistor [16]. The working principle of the ACS 712 current sensor is: current flows to the load, and a magnetic field is generated on the ACS 712 IC in the dynamic bias section, which is amplified and filtered by the amplifier, then released. ACS 712 current sensor pin function:

a. Somewhere in between. The VCC pin is the sensor voltage source;
b. The OUT pin is used as the sensor output voltage;
c. The GND pin is grounded;
d. The main terminals are connected in series with the load.

It can be seen that the output voltage is between 0-5 VDC, and the current ratio is -30A-30A, at no-load condition the sensor output voltage is 2.5 VDC and the current condition is 0 A [5].

2.5. Atmega microcontroller 16

Atmega16 microcontroller is an AVR series microcontroller. Compared with the previous MCS-51 and 52 series microcontrollers, this IC has many advantages. The advantage of the Atmega16 IC is that it already has an internal 8-bit and 10-bit ADC, so it is very suitable for applications that require sensors as a medium for reading external conditions [17]. We can use the AVR Bascom software medium to program the microcontroller in a high level language (i.e., the base language). The following is the atmega16 PIN configuration. This is a function of the Atmega16 output pins:

a. VCC is the pin used as the input power supply pin;
b. GND (ground) is the ground pin;
c. PORTA (PORTA0-7) is a two-way I / O pin, dedicated to the ADC input pin;
d. PORTB (PORTB0-7) is a two-way I / O pin with special functions, such as timer / counter pin, analog comparator and SPI;
e. PORTC (PORTC0-7) is a two-way I / O pin with a special function, namely TWI, analog comparator and oscillator timer;
f. PORTD (PORTD0-7) is a two-way I / O pin with special functions namely analog comparator, external interrupt and USART serial communication;
g. RESET is the pin used to reset the microcontroller;
h. XTAL1 and XTAL2 are external clock pins;
i. AVCC is the ADC voltage input pin;
j. AREF is the ADC reference voltage input pin.

The Atmega16 has 16GB of program flash memory. It also has 608 data storage addresses, divided into 3 parts, namely 32 public registers, 32 I / O registers and 512 byte EEPROM [6].

2.6. LCD

A liquid crystal display (LCD) is a digital display technology that produces a flat image by illuminating the liquid crystal and filtering out the color of the polar molecular structure sandwiched between two transparent electrodes. When an electric field is applied, the molecules adjust their position according to the electric field, forming a crystal arrangement that polarizes the light that passes through it [7]. The following table is a table of LCD ports.

2.7. IC Driver Motor L293D

The L293D driver IC is specially designed as a DC motor driver, which can be controlled by an analog circuit or a microcontroller. Since the DC motor controlled by the L293D IC is directly connected to the IC output, there is no need to connect it to ground or positive power supply. Since the drver system used in the L293D is four-pole, there are 4 independent DC motor drivers, each of which can consume 1A of current [9].

3. Method

3.1. System Diagram

The block diagram above can be explained as follows:

a. The LDR sends data to the brightest position under the sun;
b. The microcontroller processes it as digital data and orders the motor to rotate;
c. Enter the solar cell voltage to the regulator to reduce it to 14 volts;

d. Current sensor and battery voltage sensor, solar battery voltage sensor is sent to the microcontroller to display the measurement results;
e. The switch is used for data point setting, measurement menu setting and manual setting.

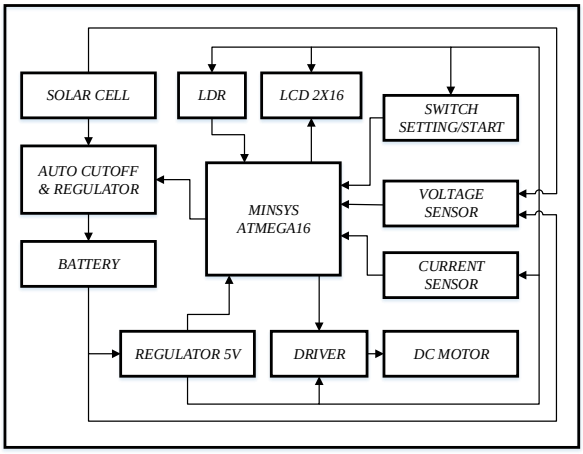

Fig. 2. System diagram

4. Results and Discussion

4.1. Hardware Design

1. Sensor and Motor Installation

In the first stage of controlling solar cell tracker hardware, the LDR is used as a sensor to receive sunlight. The microcontroller will receive a change in voltage from the LDR circuit and enter the PORT ADC position (PA0-PA3) for data processing.

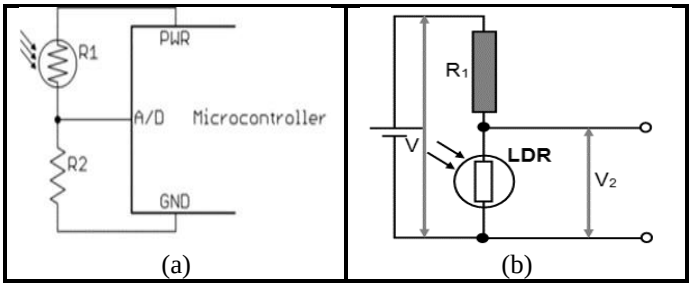

Fig. 3. (a) Wiring of the LDR connection to the microcontroller [18], (b) LDR voltage divider circuit [18]

Table 1. LDR Voltage Distributor Circuit

No.	PORT address	Variable / Usage
1	*PORT A1*	LDR sensor 1
2	*PORT A2*	LDR sensor 2
3	*PORT A3*	LDR sensor 3
4	*PORT A4*	LDR sensor 4

The motor will rotate according to the sensor command, and the motor will be connected as an output to PORTD 0-5, each motor uses 2 outputs to control the rotation intensity of motor 1 and motor 2. The following table shows the ports used:

Table 2. Use of the Motor Driver Ic Feet

No.	PORT address	Variable / Usage
1	*PORTD.0*	Motor 1 rotates clockwise
2	*PORTD.1*	Motor 2 rotates clockwise
3	*PORTD.2*	Motor 1 turn counterclockwise
4	*PORTD.3*	Motor 2 turn counterclockwise
5	*PORTD.4*	Motor speed 1

2. Installation of Current Sensor and LCD

LCD installation and connection, used to display battery voltage and current data. When connecting LCD feet, all 16 PINs will not be used. And you have to pay attention to the VCC polarity and ground voltage, the RS, E, R / W data ports should not be reversed, the maximum operating voltage of the LCD is 5V. The following image shows the LCD connection diagram:

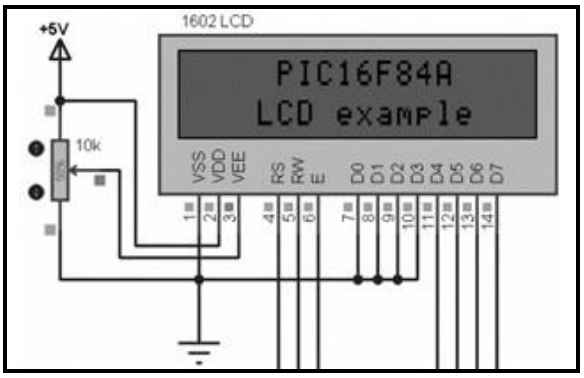

Fig. 4. Connect the LCD to the microcontroller [8]

The current sensor using the ACS 712 sensor module is connected in series between the solar cell and the battery voltage regulator, and is used as an automatic charger sensor after the battery is fully charged. The following figure shows the ACS 712 sensor connection design:

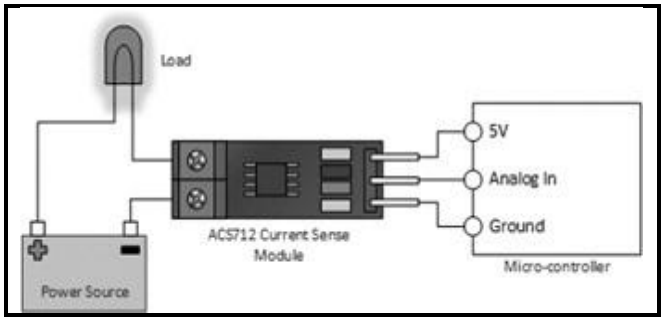

Fig. 5. Connection of AC712 current sensor [5]

It can be seen from Figure 15 that the relationship between the bulb load and the sensor can send an analog signal to a microcontroller that can display the charging current.

4.2. Testing

Compared to solar cells that do not use a control system, this system is used to control solar cells to directly face the sun to get maximum energy, so that these solar cells produce better power. By using the ATMEGA16 microcontroller, it can be monitored in the form of displays and commands, so that the status of each controlled device can be seen from the device, so data and operations can be retrieved more easily. After the system design has been completed, the next step is to test the performance of the solar cell tracker. Here are the test steps:

a. Connect all minimal systems to the power regulator, then connect the sensor, switch, LCD to the microcontroller;
b. Connect each motor to the driver, connect the battery to the regulator, then connect the solar cell to the regulator;
c. Connect the downloader to the computer with a USB cable, then connect the micro system to the downloader;
d. Run the BASCOM AVR program, then KHAZAMA will upload the created program to the minimal system;
e. Turn on the power switch to run the smallest system, regulator and motor.

The working principle of this tool is to use a manipulator that is driven by two DC motors to make the solar cell face the sun and adjust the motor movement according to the sensor's command, namely reading sunlight by logically comparing the data between the sensors.

Fig. 6. Uneven Sensor Data Display

As can be seen from the data above, the result of reading the data from the LDR sensor to the uneven LCD screen is used as a rotating motor command.

Fig. 7. Sensor Data Showing Unevenness

From the data above, you can see the result of reading the data from the LDR sensor to the same LCD screen, which is used as a motor command to stop facing the sun.

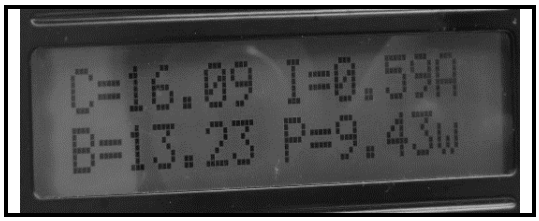

Fig. 8. Measurement Display

Display C is the solar battery voltage, display I is the current when the battery is charging, display B is the battery voltage status, and P is the current power state. The charging current is displayed as 0.59A. If the charging current is less than "0" or negative, the charging process is not carried out.

4.3. Results

Table 3. Passive and Tracker Solar Cell Testing Day 1

Average Result	Passive Solar Cell	Solar Cell Tracker
Current (A)	0,57	0,69
Voltage (V)	15,64	15,72
Power (W)	8,73	10,79
Beam Angle (°)	2,25	-
Battery Voltage (V)	12,72	12,79

Table 4. The Difference Between Solar Cell Passive and Solar Cell Tracker on Day 1

DIFFERENCE			Percentage of Increase (%)		
Charge Current (A)	Charge Voltage (V)	Charge Power (W)	Charge Current (A)	Charge Voltage (V)	Charge Power (W)
0,12	0,08	2,06	21,05%	0,51%	23,59%

From the data table above, testing was carried out on the first day of an increase in power of 23.59%, a voltage of 0.51% and a current of 21.05%. By using a 12V 12 lamp load and tracker control.

Table 5. Passive and Tracker Solar Cell Testing Day 2

Average Result	Passive Solar Cell	Solar Cell Tracker
Current (A)	0,50	0,66
Voltage (V)	15,64	15,81
Power (W)	7,87	10,39
Beam Angle (°)	2,25	-
Battery Voltage (V)	12,69	12,83

Table 6. The Difference Between Solar Cell Passive and Solar Cell Tracker on Day 2

DIFFERENCE			Percentage of Increase (%)		
Charge Current (A)	Charge Voltage (V)	Charge Power (W)	Charge Current (A)	Charge Voltage (V)	Charge Power (W)
0,16	0,17	2,52	32,00%	1,08%	32,02%

Based on the data sheet above, the test was carried out on the first day, the power increased by 32.02%, the voltage increased by 1.08%, and the current increased by 32.00%. By using a 12V 12 lamp load and tracer control.

Table 7. Passive and Tracker Solar Cell Testing Day 3

Average Result	Passive Solar Cell	Solar Cell Tracker
Current (A)	0,58	0,73
Voltage (V)	15,51	15,62
Power (W)	9,07	11,38
Beam Angle (°)	2,25	-
Battery Voltage (V)	12,34	12,59

Table 8. The Difference Between Solar Cell Passive And Solar Cell Tracker on Day 3

DIFFERENCE			Percentage of Increase (%)		
Charge Current (A)	Charge Voltage (V)	Charge Power (W)	Charge Current (A)	Charge Voltage (V)	Charge Power (W)
0,15	0,11	2,31	25,86%	0,70%	25,46%

Based on the data sheet above, the test was carried out on the first day of testing, the power increased by 25.46%, the voltage increased by 0.70%, and the current increased by 25.86%. By using a 12V 12 lamp load and tracer control.

In the three test results, the ratio of solar cells to the passive system is tilted 45 degrees to the north, and the comparison of solar cells using a tracker shows that August 10 to August 13, 2020 is morning to noon. In the test results, data is retrieved every 30 minute, and the amount of data increases 10-fold. Comparing the difference, the power supply side is 27,02%, the voltage side is 0,76%, and the charging current side is 26.30%.

Table 9. Percentage of Average Test Results for 3 Days

TOTAL 3 TIMES OF TESTING (%)			TESTING AVERAGE 3 TIMES (%)		
Charge Current (A)	Charge Voltage (V)	Charge Power (W)	Charge Current (A)	Charge Voltage (V)	Charge Power (W)
78,91%	2,29%	81,07%	26,30%	0,76%	27,02%

Passive solar cells tend to face straight 45° north, while active solar cells follow sunlight. In terms of getting the same angle of sunlight, the equation is:

$$\omega = \frac{(T_s - 10)\ x\ 360}{24} \quad (1)$$

Can be determined the angle of the sun for a passive or active position. You can see the angle every 30 minutes along with the chart conditions with the reference at 10:00 a point of 0 degrees is made.

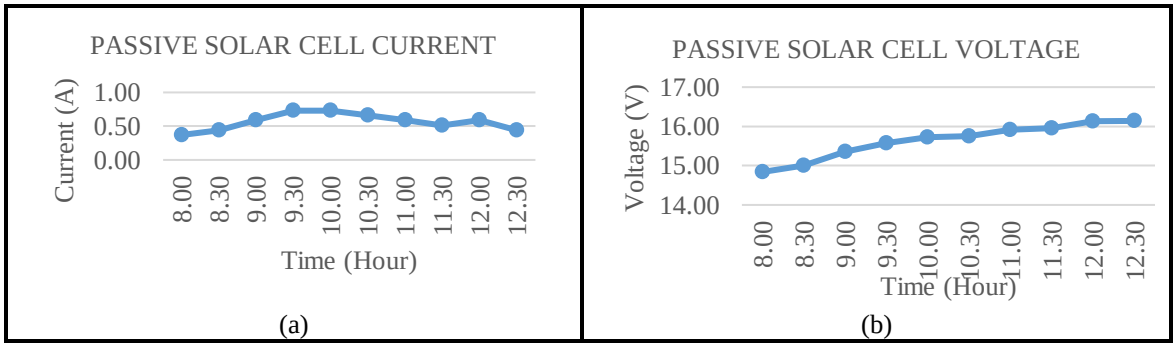

Fig. 9. (a) Current chart of passive solar cells on test day 1, (b) Voltage chart of passive solar cells on test day 1

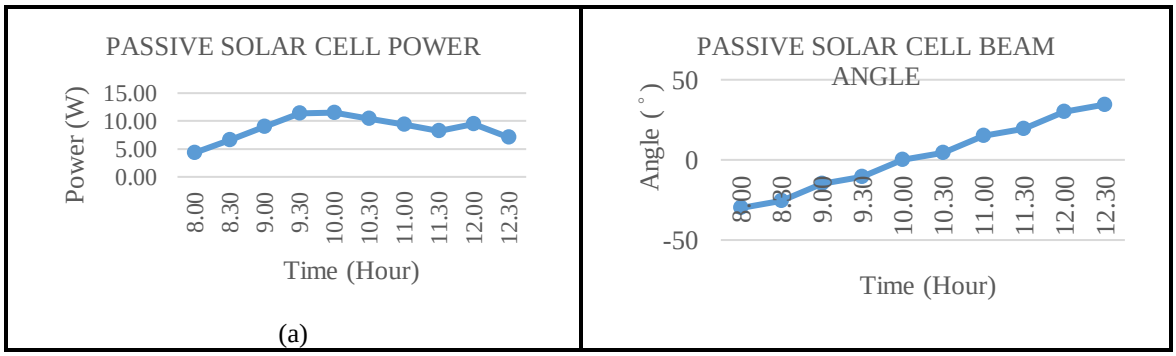

Fig. 10. (a) Graph of passive solar cell power on test day 1, (b) Angular graph of passive solar cells on test day 1

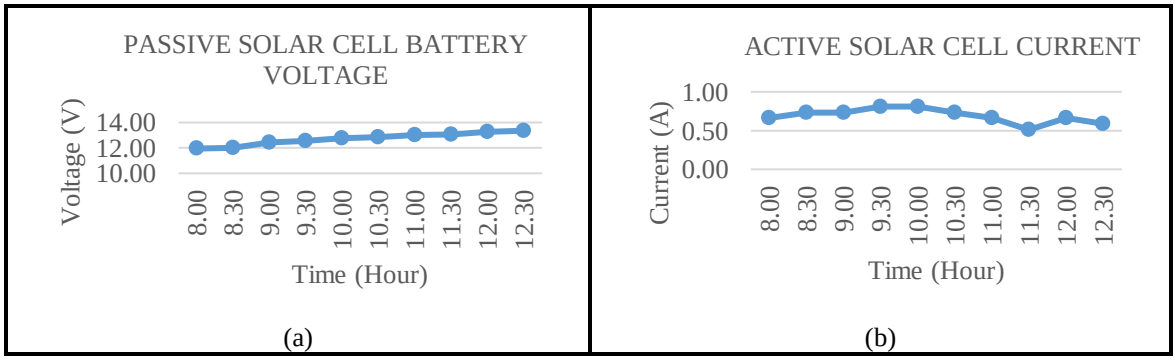

Fig. 11. (a) Graph of passive solar cell battery voltage on test day 1, (b) Current chart of active solar cells on test day 1

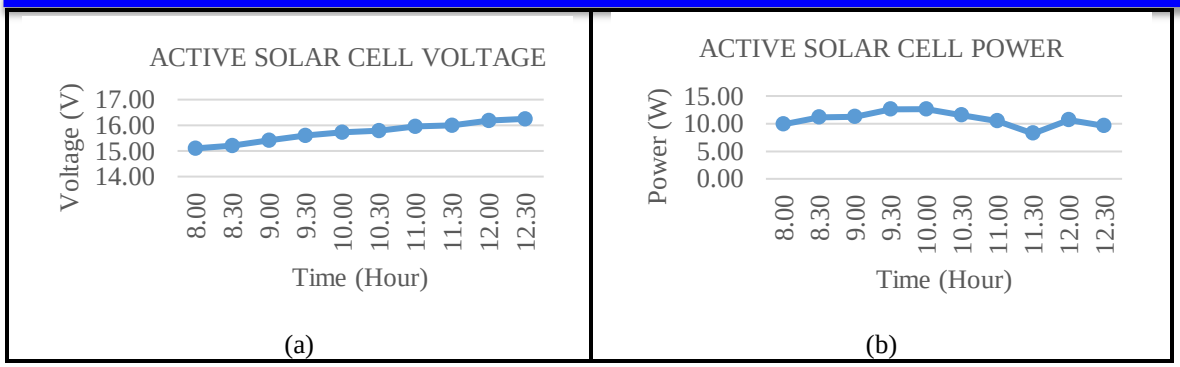

Fig. 12. (a) Graph of active solar cell voltage on test day 1, (b) Graph of active solar cell power on test day 1

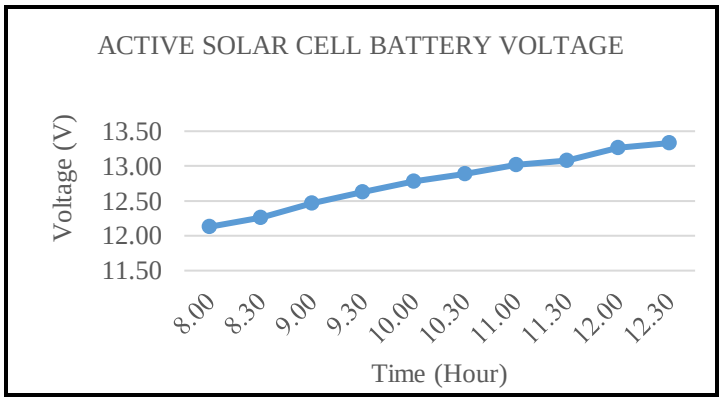

Fig. 13. Graph of active solar cell battery voltage on test day 1

From the test charts on the first day, it can be seen the difference between the increase in passive solar panels and active solar panels. Active solar panels can absorb sunlight more effectively so that they get 0.12A charge current, 0.08V charge voltage, and 2.06W more charge than passive solar panels.

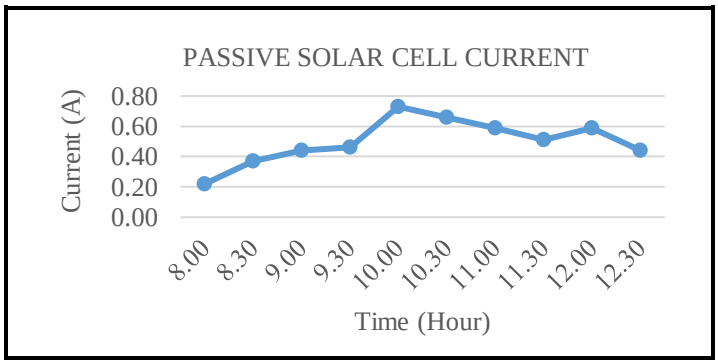

Fig. 14. Current chart of passive solar cells on the second day of testing

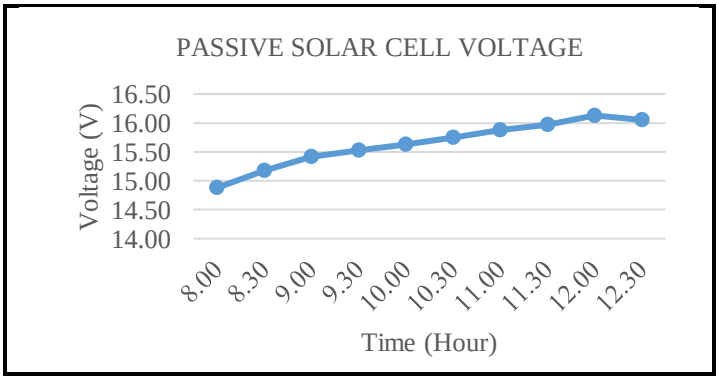

Fig. 15. Graph of passive solar cell voltage on the second day of testing

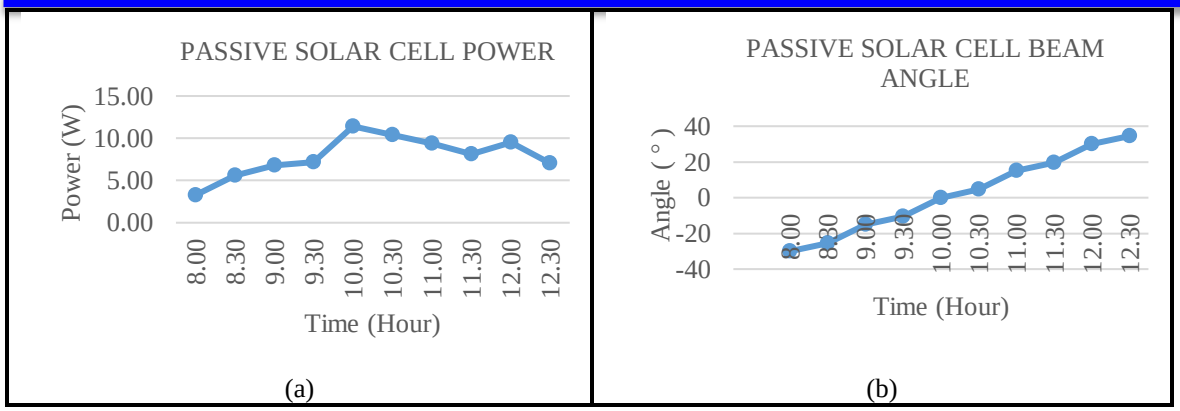

Fig. 16. (a) Graph of passive solar cell power on the second day of testing, (b) Angular graph of passive solar cells on the second day of testing

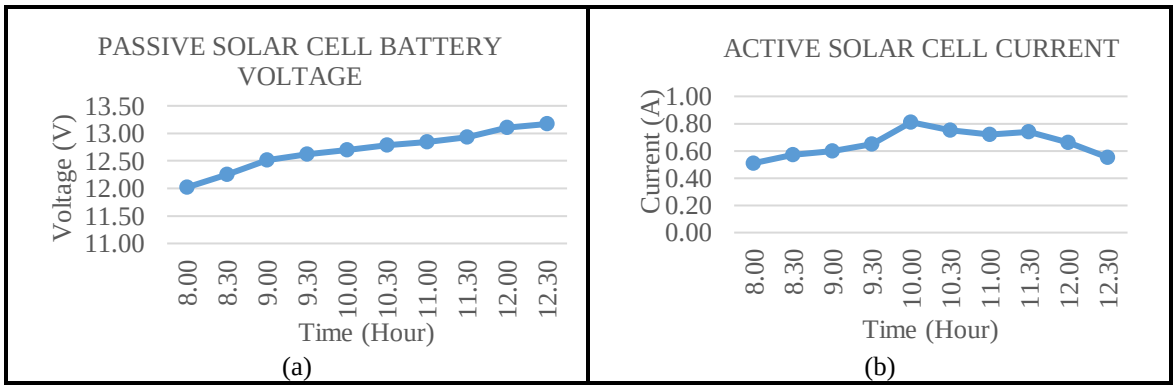

Fig. 17. (a) Graph of passive solar cell battery voltage on the second day of testing, (b) Current chart of active solar cells on the second day of testing

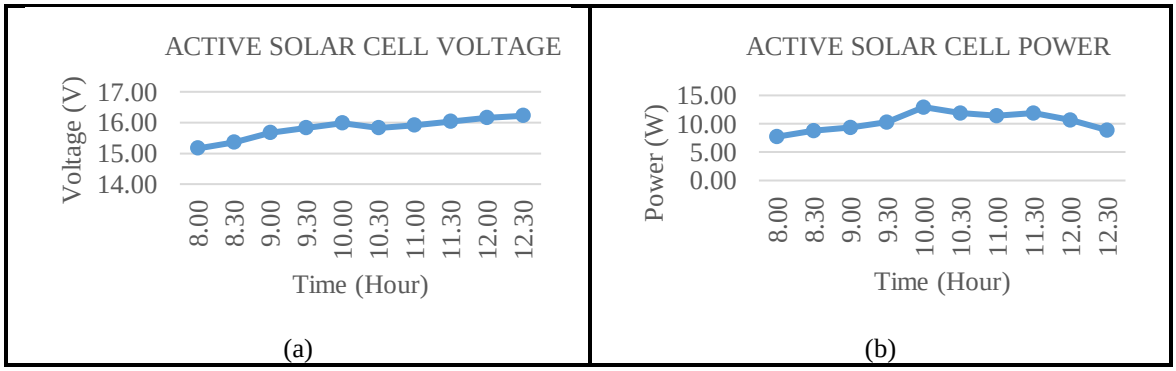

Fig. 18. (a) Graph of active solar cell voltage on the second day of testing, (b) Graph of active solar cell power on the second day of testing

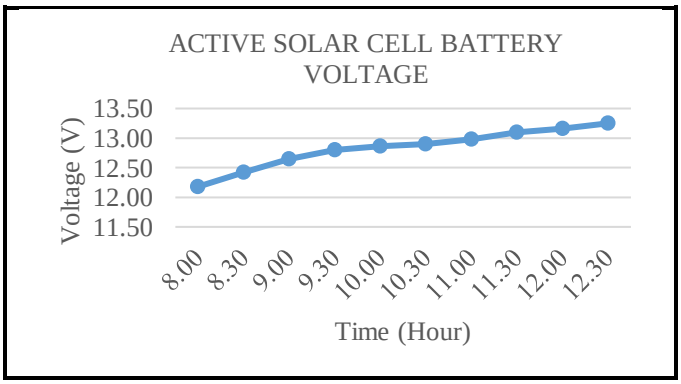

Fig. 19. Graph of active solar cell battery voltage on the second day of testing

From the graphs of the second day of testing, there is a difference between the increase in passive solar panels and active solar panels. Active solar panels can absorb sunlight more effectively so that they get 0.16A charge current, 0.17V charge voltage, and 2.52W more charge than passive solar panels.

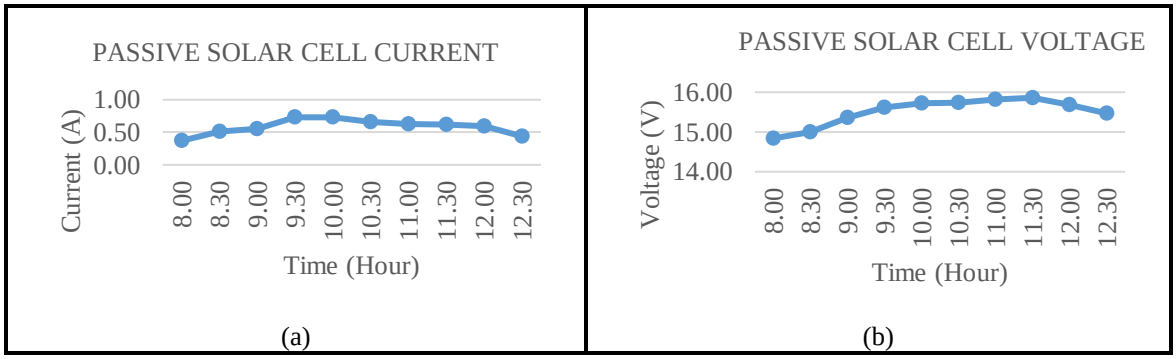

Fig. 20. (a) Current chart of passive solar cells on the 3rd day of testing, (b) Graph of passive solar cell voltage on the 3rd day of testing

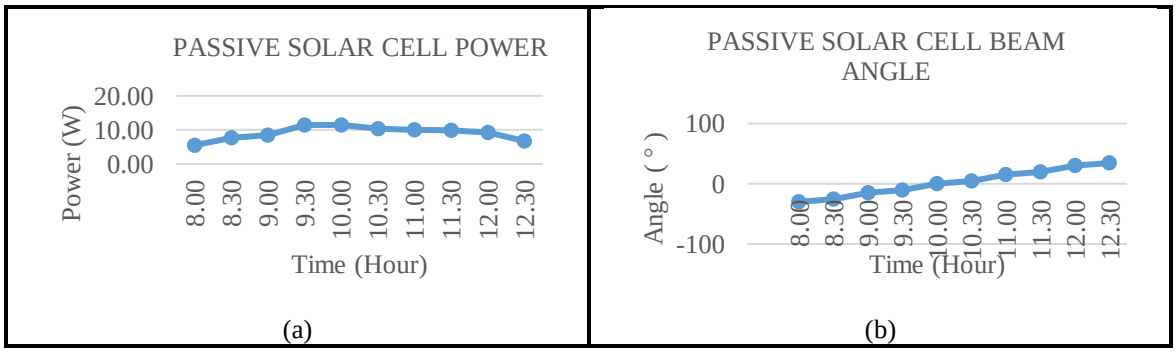

Fig. 21. (a) Graph of passive solar cell voltage on the 3rd day of testing, (b) Angular graph of passive solar cells on the 3rd day of testing

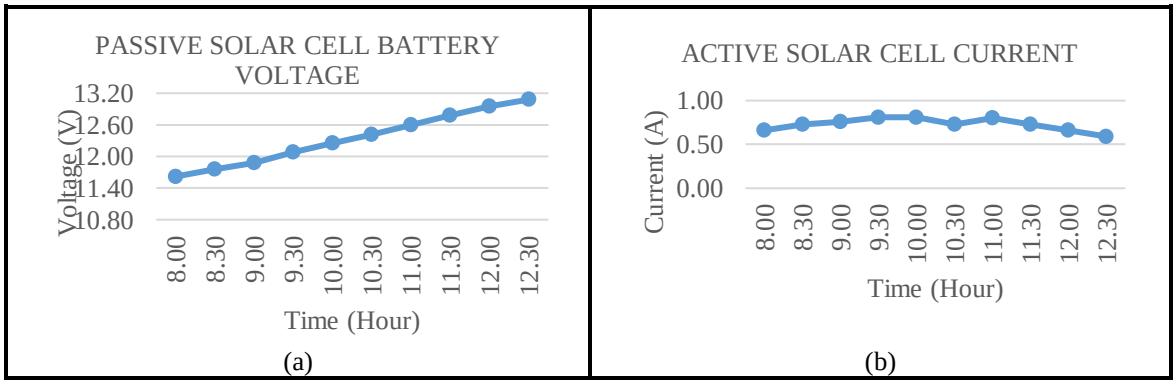

Fig. 22. (a) Graph of passive solar cell battery voltage on the 3rd day of testing, (b) Current chart of active solar cells on the 3rd day of testing

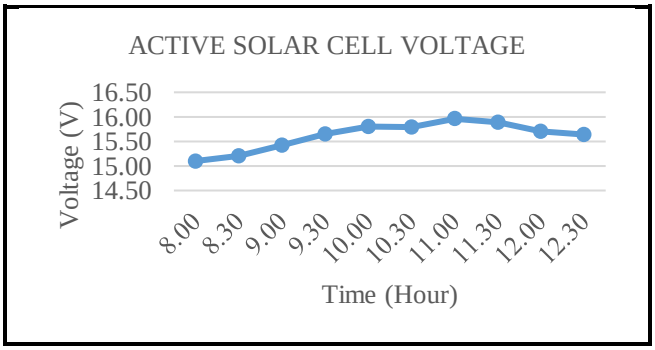

Fig. 23. Graph of active solar cell power on the 3rd day of testing

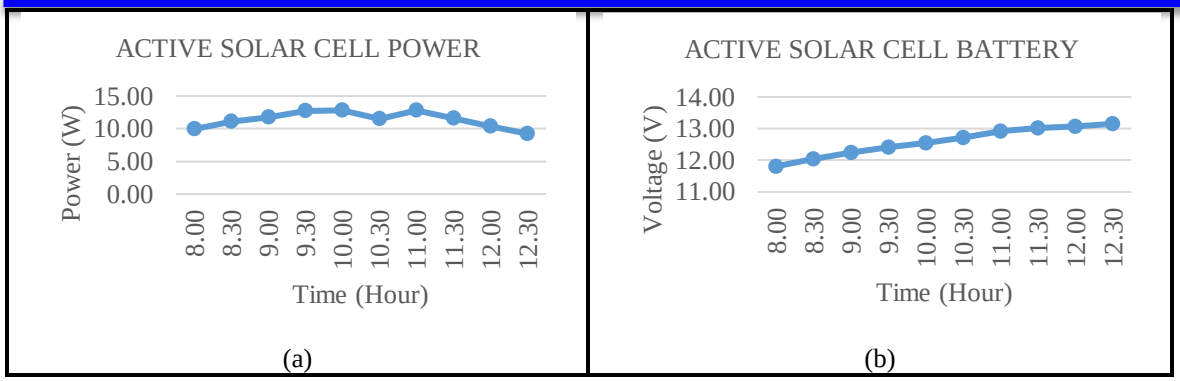

Fig. 24. (a) Graph of active solar cell power on the 3rd day of testing, (b) Graph of active solar cell battery voltage on the 3rd day of testing

From the test charts for the third day, it can be seen the difference between the increase in passive solar panels and active solar panels. Active solar panels can absorb sunlight more effectively so that they get 0.15A charge current, 0.11V charge voltage, and 2.31W more charge than passive solar panels.

Fig. 25. Position of the Solar Tracker at 12.00

The prototype mentioned in this article is based on the design and implementation of an inexpensive and effective sensor-activated sun tracking device that uses a light sensor to detect sunlight. The microcontroller reads the measured intensity as input and instructs the actuator to change the position of the sensor.

From looking for some articles on making solar cells to increasing efficiency, we just need to look for materials that can absorb the maximum ultraviolet photons and look for the static angle of solar cells. However, an automatic solar tracker is a tracker whose solar panels will move to follow the movement of sunlight, so that it is expected to absorb light properly. go. Therefore, the solar cell panel material has a longer service life.

Fig. 26. Position of the Solar Tracker at 9.30

Manufacturers are constantly upgrading their solar panels to produce higher unit energy yields than previous competing products and similar products. Another effective way to increase system output is to use a solar tracker, which is different from a fixed inclined ground-mounted system that allows solar panels to follow the sun's path throughout the day. There are two types of solar trackers on the market: single axis and double axis. A single axis solar tracker tracks the sun from east to west, rotates at a single point, and moves synchronously according to rows of panels or segments. The dual-axis tracer rotates on the X and Y axes simultaneously, so the panel is directly tracking the sun. Sun Trackers A single axis tracer tracks the sun from east to west at a single point.

Compared to dual axis trackers, single axis trackers will collect less energy per unit, however due to their shorter shelf height they require less installation space, which makes the system more centralized and easier to operate and maintain.

There are two types of single axis tracers: centralized and distributed. Centralized or distributed trackers use a single electric motor to power the inter-line transmission system, which drives the entire panel. Each tracer line of the decentralized system has an electric motor. There are tracer instances in each rack group, and each rack has a motor, which causes more rows during installation. In some cases, they can be used to track independently of neighboring modules.

Single axis solar trackers were originally designed to work like blinds, with entire rows of panels moving at the same time throughout the day. It is now being considered built into the tracking software so that the panel lines can compensate for scattered light, unfavorable wind conditions, and horizontal and horizontal shadows.

On a dark cloud day, sunlight does not reach the earth's surface through direct light, but is received in the form of scattered light, meaning the panels facing the sun may not produce the most light. This may mean that the panels will be positioned horizontally to capture the scattered light.

5. Conclusion

Based on the results of the design and testing that has been completed, the following conclusions can be drawn: Install a sensor screen to speed up response to daytime motion. The final power efficiency tracker is best used in the morning because it is relatively close during the day. By using a suitable power source between charging and discharging, the battery can still be fully charged. Compared to passive solar cells, the use of tracers to install solar cells can obtain a higher capacity, namely 27.02%, with the arrival of sunlight, the angle o f acceptance of solar cells is 90°.

References

[1] Poulek, V., and M. Libra. "A very simple solar tracker for space and terrestrial applications." Solar Energy Materials and Solar Cells 60.2 (2000): 99-103.

[2] Nugraha, A. T., & Priyambodo, D. (2021). Design of a Monitoring System for Hydroganics based on Arduino Uno R3 to Realize Sustainable Development Goals number 2 Zero Hunger. Journal of Electronics, Electromedical Engineering, and Medical Informatics, 3(1), 50-56..

[3] F. Afifudin and F. S. Hananto, “SOLAR CELL MENGGUNAKAN LENSA PEMFOKUS.”H. Jin and B. Miao, “Design of Holter ECG system based on MSP430 and USB technology,” 2007 1st Int. Conf. Bioinforma. Biomed. Eng. ICBBE, pp. 976–979, 2007.

[4] E. B. Raharjo and I. Setiawan, “MENGGUNAKAN MIKROKONTROLER ATMEGA8535,” pp. 1–10.

[5] "ACS712 Module Measures Currents up to 30A for as Low as $1 Shipped.".

[6] K. I. Sram, “with 16K Bytes Programmable ATmega16 (L).”.

[7] D. Electronic, “M1632 module lcd 16 x 2 baris (m1632),” no. 0100 0001.

[8] Nugraha, Anggara Trisna, and Dadang Priyambodo. "Development of Rocket Telemetry in Chamber Gas Pressure Monitoring with the MPXV7002DP Gas Pressure Sensor." Journal of Electronics, Electromedical Engineering, and Medical Informatics 2.3 (2020): 103-107.

[9] D. Information, “L293x Quadruple Half-H Drivers,” 2016.

[10] Poulek, Vladislav, and Martin Libra. "New solar tracker." Solar energy materials and solar cells 51.2 (1998): 113-120.

[11] Tudorache, Tiberiu, and Liviu Kreindler. "Design of a solar tracker system for PV power plants." Acta Polytechnica Hungarica 7.1 (2010): 23-39.

[12] Nugraha, Anggara Trisna, Mayda Zita Aliem Tiwana, and Alwy Muhammad Ravi. "Analisis Optimalisasi Manajemen Daya Chiller Untuk Rencana AC Sentral Industri." Jurnal Janitra Informatika dan Sistem Informasi 1.1 (2021): 35-46.

[13] Chin, C. S., A. Babu, and W. McBride. "Design, modeling and testing of a standalone single axis active solar tracker using MATLAB/Simulink." Renewable Energy 36.11 (2011): 3075-3090.

[14] Umanand, Prof. L., 2007, Non-Conventional Energy Systems. Bangalore : Indian Institute of Science Bangalore.

[15] Tong, C.W., 1997, The Design And Testing Of A Wind Turbin For Malaysian Wind Condition, thesis, UTM.

[16] Pikatan, Sugata., 1999, Konversi Energi Angin. Surabaya : Departemen Mipa Universitas Surabaya.

[17] Anonim 3, 2012, Keuntungan Kerugian Angin, (Sumber : www.surya.co.id), di unduh pada tanggal 21 April 2012 pukul 08.30 wita.

[18] Manwell, J.F ., 2002. Wind Energy Explained Theory, Design and Application. Amherst : John Wiley and Sons, Ltd.